Soft Matter

Formation of Ion Gels by Polymerization of Block Copolymer/Ionic Liquid/Oil Mesophases

Journal:	*Soft Matter*
Manuscript ID	SM-ART-05-2020-000850.R1
Article Type:	Paper
Date Submitted by the Author:	03-Jun-2020
Complete List of Authors:	Bandegi, Alireza; New Mexico State University, Chemical and Materials Engineering Banuelos, Jose; University of Texas at El Paso, Physics Foudazi, Reza; New Mexico State University, Chemical and Materials Engineering

Formation of Ion Gels by Polymerization of Block Copolymer/Ionic Liquid/Oil Mesophases

Alireza Bandegi [a], Jose L. Bañuelos [b], Reza Foudazi [a*]

[a] Department of Chemical and Materials Engineering, New Mexico State University, Las Cruces, NM, 88003, United States

[b] Department of Physics, The University of Texas at El Paso, El Paso, TX, 79968, United States

[*] Corresponding author. Email: rfoudazi@nmsu.edu.

Abstract

In this study, we introduce a new way of developing ion gels through polymerization of lyotropic liquid crystal (LLC) templates of monomer (styrene), cross-linker (divinylbenzene), ionic liquid (1-ethyl-3-methylimidazolium tetrafluoroborate), and amphiphilic block copolymers (Pluronic F127). The polymerization of oil phase boosts the mechanical properties of the ion-conducting electrolytes. We discuss the effect of tortuosity induced by crystalline domains and LLC structure on the conductivity of ion gels. The ion transport in polymerized LLCs (polyLLCs) can be controlled by changing the composition of the mesophases. Increasing the block copolymer concentration enhances the crystallinity of PEO blocks in the conductive domains, which slow down dynamics of PEO chain and ion transport. We show that by adjusting the composition of LLC mesophases, the mechanical strength of ion gels can be increased one order of magnitude without compromising the ionic conductivity. The polyLLCs with 45/25/30 wt% (block copolymer/IL/oil) composition has storage modulus and ionic conductivity higher than 1 MPa and 3 mS/cm at 70 ˚C, respectively. The results suggest that LLC templating is a promising method to develop highly conductive ion gels, which provides advantages in terms of variety and processing.

Introduction

Ionic liquids (ILs) have attracted significant interest due to their unique properties including high thermal stability, negligible vapor pressure, wide electrochemical window, and high ionic conductivity and specific capacitance.[1–3] To enhance the practicality of employing ILs in different applications, it is important to blend them with structuring polymers to form physically or chemically crosslinked networks. The resulting network is referred to as ion gel.[4–7] Ion gels can overcome the leakage and flammability issues of organic solvent-based electrolytes and have shown tunable mechanical behavior and high ionic conductivities,[8–12] which enable extensive applications in different areas including dye-synthesized solar cell (DSSCs),[13,14] electrolyte gate transistors (EGTs),[15–24] electrochemical displays,[25–28] supercapacitors,[29,30] and gas separation membranes.[31,32] In addition, ion gels are solution processable and compatible with high throughput patterning methods (e.g., printing).

Chemically cross-linked Ion gels can be obtained by linking the polymer chains through covalent bonds.[4,6,33,34] Physically cross-linked ion gels can be prepared by using block copolymers (BCPs) that are partially compatible with ionic liquids.[35–39] For example, by combining a few weight percent of the triblock copolymer ABA, where the A end blocks are insoluble and the B middle block is soluble in an ionic liquid, a soft gels can be obtained.[5] Using block copolymers as polymer matrix provides the opportunities to control the gel structure and physical properties through variation of the copolymer block lengths, architecture, or identities.[36,40] However, a disadvantage of physical gels is low modulus due to chain pull out from the microphase separated domains of immiscible block.[5]

One important challenge towards the implementation of ion gel in large-scale systems is to enhance their mechanical strength without compromising the ionic conductivity.[41] The development of heterogeneous electrolytes, comprising ion-rich and ion-poor regions, has enabled the decoupling of electrical and mechanical properties. The most common method used to achieve this decoupling is to utilize the self-assembled structures of BCPs.[42] Through the self-assembly process, BCPs create various nanoscale morphologies, such as spheres, cylinders, gyroids, or lamellae.[43,44] A hybrid electrolyte with conductive and nonconductive microdomains can be made due to the high affinity of ILs to the miscible block in BCPs. Several works have been reported on the morphology, ionic conductivity, glass transition temperature, and tensile strength of binary IL/BCP mixed systems as function of the IL content.[45–51] Incorporating ILs into the conducting domains of the heterogeneous ion gels significantly increases the ionic conductivity. However, the presence of large amounts of IL deteriorates the mechanical strength of the polymer gel electrolyte. The conductivity of microphase-separated ion-conducting BCPs is dependent on nanoscale morphology and the degree of connectivity of ionic domains.[51–56] It has been suggested that strong microphases separation[57–59] and large microdomain width[57,60] favor high conductivity.

In the presence of selective solvent(s), amphiphilic BCPs self-assemble into ordered mesomorphic structures (known as mesophases) with long-range order. By altering the temperature and concentration, a variety of nanostructures, such as lamellar, hexagonal, cubic, and gyroid structures, can be formed.[51,61–67] The ordered mesophases are also referred to as lyotropic liquid crystals (LLCs). Because of weak mechanical strength and thermal stability, the application of LLCs was previously limited. However, by using

various amphiphilic and crosslinking monomers, more robust polymer materials with nanoscale structures have recently been obtained.[68–72] By using templates of LLCs with conventional monomers, ordered nanostructures of cross-linked networks (polymerized LLCs or polyLLCs) can be obtained if the structure is retained.[73–76] In our previous, work we showed that polyLLCs of surfactant/water/oil enable the formation of nanostructured polymers that exhibit enhanced physical properties when the original structure is retained after polymerization.[62,77]

In this work, we use the triblock copolymer (known as Pluronic) of poly(ethylene oxide)-poly(propylene oxide)-poly(ethylene oxide), PEO-PPO-PEO, as surfactant in LLCs for producing ion gels. To prepare the heterogeneous ion gels, we use ternary system of Pluronic/IL/oil mesophases. The ion gels are prepared through polymerization of mesophase templates of monomer (as oil phase), IL, and amphiphilic block copolymers. The polymerization of oil phase boosts the mechanical properties of the ion-conducting electrolyte. We show that IL-containing LLCs can be used as template to synthesize gel electrolytes with controllable mechanical strength and ionic conductivity. We also study the PEO/IL homogeneous electrolytes and Pluronic/IL binary LLCs as control samples. The effects of mesophase composition on the mechanical properties and ionic conductivity are studied to understand the role of crystallinity degree on the conductivity of polyLLCs. Improving the efficiency and scalability of the ion gel via appropriate selection of mesophase composition is the ultimate goal of this approach.

Experimental

Materials

Poly[(ethylene oxide)$_{100}$-block-(propylene oxide)$_{65}$-block-(ethylene oxide)$_{100}$] known as Pluronic F127 (Mw=12600 g/mol, PDI=1.4) was kindly provided by BASF. The polyethylene oxide (M_w=4000 g/mol, PDI=1.05), which has the same molecular weight of PEO block in F127, was used for the preparation of control samples. Styrene (≥99%, Sigma-Aldrich) and divinylbenzene (DVB) (technical grade, 80%, Sigma-Aldrich) were used as monomer and crosslinker, respectively. Azobisisobutyronitrile (AIBN, 98%, Sigma-Aldrich) was used as thermal initiator. 1-Ethyl-3-methylimidazolium tetrafluoroborate (EMIMBF4, 98%, Sigma-Aldrich) was used as ionic liquid. All chemicals were used as received without further purification. For preparation of mesophases, desired amounts of components were mixed manually until a homogeneous mesophase was obtained. The crosslinker and initiator concentrations of 50 and 3 wt% of monomer were used in all samples, respectively. The compositions were selected in a way that mesostructures with different domain sizes were obtained. The polymerization of the mesophases was done in an oven at 70 °C for 24 hours. The degree of conversion in polyLLCs is about 90%.[62] As control samples, homogeneous (PEO/IL) and heterogeneous (Pluronic/IL) electrolytes were prepared with the same ratio of PEO/IL as in the mesophase samples.

X-ray Scattering

Small angle X-ray scattering (SAXS) and wide-angle X-ray scattering (WAXS) were used to confirm mesostructure and crystallinity degree of each sample, respectively. SAXS measurements were carried out using a Xeuss 2.0 HR SAXS/WAXS system with a Cu source tuned to λ = 0.1542 nm and at two sample detector distances (156 mm and 1215

mm) to span a *q*-range of 0.006-2.6 $Å^{-1}$. The mesophases were placed into a Teflon ring, which held the samples at a constant diameter (6 mm) and thickness (1 mm) and then polymerized under press in oven at 70 °C for 24 hours. Then, the samples were placed in SAXS instrument for measurement. It was shown in our previous works that the mesophases structure is retained after polymerization when sufficient amount of crosslinker is used.[77,78] Therefore, all the SAXS measurements in this work were done at room temperature after complete polymerization of the samples at 70 °C.

Differential Scanning Calorimetry

For measuring the thermal properties of samples, differential scanning calorimetry (DSC) was carried out by Q2000 DSC from TA Instruments (New Castle, DE). About 10 mg of samples was placed in a Tzero aluminum pan and sealed with Tzero hermetic lid. All measurements were performed under a nitrogen gas atmosphere. The thermal properties of the samples were then measured using a heat-quench-heat method: for measuring the crystallinity degree at 20 °C, the samples were equilibrated at 70 °C, held isothermally for 10 min, cooled down to 20 °C at 2 °C/min, held isothermally for 10 min, and then heated back up to 70 °C at 2 °C/min. The analysis of thermograms was performed using the TA Instruments Universal Analysis 2000 software: melting transitions were analyzed using the “Peak Integrate Linear” function. Heats of fusion were estimated from the endotherm of the second heating and the weight fraction of PEO incorporated into the polymer electrolytes. Percent crystallinity was calculated in reference to the enthalpy of 203.4 J/g for pure crystalline PEO.[79] Melting temperatures (T_m’s) are reported from the peak temperature values.

157

158 **AC Impedance Spectroscopy**

159 The ionic conductivity was measured via electrochemical impedance spectroscopy (EIS).
160 The mesophases were placed into a Teflon ring, which held the samples at a constant
161 diameter (6 mm) and thickness (2 mm) and then polymerized under press in oven at 70
162 °C for 24 hours. The sample disks were sandwiched between two stainless steel blocking
163 electrodes. Sample temperature was maintained using a custom-built environmental
164 chamber. The samples were held at each temperature for 1 h before measurement. The
165 AC amplitude was 50 mV and the frequency were scanned from 1 MHz to 0.1 Hz. The
166 conductivity of the samples was calculated from the complex impedance ($Z^* = Z' - iZ''$).
167 The high-frequency plateau in the real impedance (Z') was taken as the bulk resistance
168 (R) of the sample, and the conductivity was calculated as follows:

169 $$\sigma = \frac{\mathrm{L}}{\mathrm{RA}} \quad (1)$$

170 where L is the sample thickness and A is the electrode contact area.

171

172 **Rheology**

173 A stress-controlled rheometer DHR-3 (TA Instruments, New Castle, DE) was used to
174 study the mechanical strength of the gel electrolytes. A 20 mm cross-hatched parallel
175 plate geometry (to suppress the wall-slip; it should be noted that our recent work shows
176 the wall-slip is negligible in uncured mesophases[61]) with 1 mm gap was used in all
177 experiments. A solvent trap filled with DI water was used to minimize the monomer loss
178 during polymerization under rheometer. All tests are performed in the linear viscoelastic

region (0.5% strain, confirmed from amplitude sweep tests). Time tests in small amplitude oscillatory shear mode were done on mesophases at 70 ºC at constant frequency of 1 Hz. The final plateau at storage modulus is considered as mechanical strength[62] of the polymer electrolytes.

Results and Discussion

SAXS analysis

Five different ternary mesophases were investigated with different concentrations of Pluronic and ionic liquid to deconvolute the roles of composition and overall ionic content on conductivity. In addition, two binary systems with Pluronic/ionic liquid mixture were prepared as control samples to investigate the effect of oil phases on final performance of the polymer electrolyte. The interaction between the imidazolium and ether oxygen can enhance the miscibility of the IL with PPO. However, the methyl group on the PPO chain shields this interaction as it has been reported that the IL is immiscible with PPO.[67] It is also well known that the Imidazolium based ionic liquids are not soluble in styrene.[51,80] Therefore, it is reasonable to assume that the amphiphilic block copolymer self-assembles at the interface of styrene and IL phases.

The SAXS pattern of polymerized mesophases are shown in Figure 1. There are strong peaks in the SAXS profiles with q ratio of 1:2, while no peak beyond 2q* is detected. A similar pattern is observed by Ning Zhou and coworkers in developing a ternary polymer system to study the phase behavior near the bicontinuous microemulsion phase regime.[81] They observed only two scattering peaks with q* ratio of 1:2 using Cu Ka SAXS patterns. It was shown that the broad, second, higher-order peak obtained in the relatively low-

resolution techniques actually split into two clear peaks at $\sqrt{3}q^*$ and $2q^*$ in the high-resolution synchrotron SAXS.[81] Therefore, samples studied in the current work can consist of ordered lamellar or hexagonal structure. By increasing the concentration of Pluronic in the system, the SAXS peaks shift to the left, which indicates an increase in domain spacing of the samples.

The principal scattering peaks, q*, at low q is broad. A similar broad peak is observed by Schulze and coworkers[82] using polymerization-induced phase separation (PIPS) to generate nanostructured solid polymer electrolytes. They attributed this broad peak to microphase-separated, but disordered structure. In another work, Vidil and coworkers[83] prepared robust bicontinuous nanostructured materials by exploiting the well-known order-disorder transition (ODT) of block copolymers. A single broad scattering peak was observed in their SAXS results above the ODT, which was attributed to the microphase-separated, but disorganized structure.[83] Therefore, a microphase-separated disordered structure may exist in studied ion gels in this work.

There is also a low q-scattering shouldered peak before the first peak in SAXS patterns. The large low-q intensity suggests the presence of a heterogeneity in the samples.[84] Schultz[85] attributed this low-q feature to a large (greater than lamellar length scales) individual amorphous domain inserted into the stacks of several lamellae, creating a gap in the lamellar stacks. Similar trend has been observed in ionomers.[86,87] For example, Li et al. observed a shouldered peak in the Ultra-SAXS spectra of sulfonated polystyrene ionomers and attributed its origin to polydispersity and irregularity in structure.[88] Ford and coworkers also observed the low q shouldered peak in single-ion conducting polymer electrolytes prepared from crosslinked poly(ethylene glycol)-dimethacrylate-styrene

sulfonate. They proposed that this peak is an indicative of the length scale at which the inhomogeneity becomes important from a scattering perspective.[89] In our samples, the observed shouldered peak can be attributed to an inhomogeneous structure which is induced by crosslinked disorganized domains or crystalline PEO domains in the samples. The peak position is more pronounced in Figure S6, which shows the plot of q^2I versus q (Lorentzian corrected plot) for polymer gel electrolytes in low q range, 0.005-0.02 $Å^{-1}$. The length scale of the disorganized domains is calculated from Bragg equation and it is in the range of 40-100 nm.

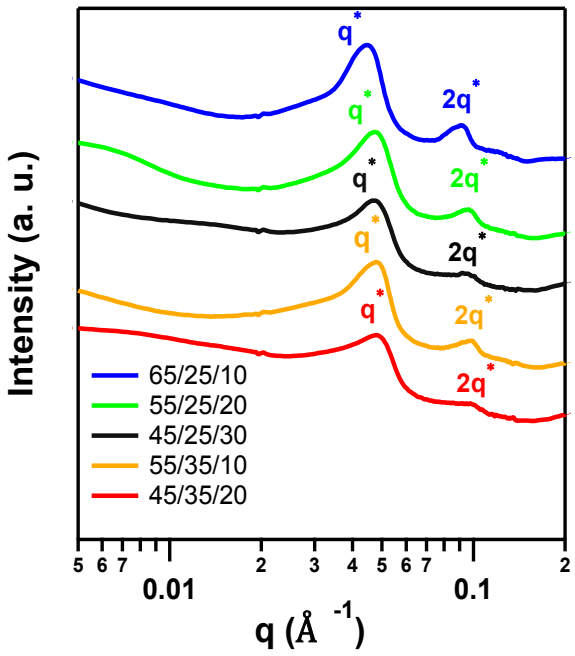

Figure 1. SAXS profiles for the polymer electrolytes with formulation of (a) F127/IL/oil wt% at room temperature (25 °C)

Ionic Conductivity

The ionic conductivity of the polymerized mesophases were measured to demonstrate the effect of composition and IL concentration on ionic conductivity of the polymer

electrolytes. Our mesophase systems provide a clear picture of how crystallinity affects ion transport in semi crystalline gel polymer electrolytes. The two factors that restrict ion conduction, tortuosity and chain dynamics, can be decoupled and quantified by controlling the crystalline morphology. For all samples as shown in Figure 2, the conductivity is enhanced by increasing the temperature. A large change of slope exists at 3.1 of 1000/T axis, which is around the melting point (T_m) of PEO. Therefore, two regimes of conduction, above and below the T_m of PEO, are apparent in the conductivity results. In all samples, a strongly non-Arrhenius behavior was observed above the T_m. Such behavior is attributed to the coupling of ion transport with polymer segmental dynamics.[90,91] However, below the T_m the conductivity shows an Arrhenius behavior and gradually increase with the temperature. The existence of crystalline domains in PEO below T_m slows down the movement of small chain segments (i.e., segmental motion). In other words, the amorphous regions are restricted by crystalline domains below T_m. Since the crystalline regions are completely absent above the T_m, a relatively high extent of segmental motion is expected, which results in high ionic conductivity.[92] The segmental motion either allows the ions to be hopped from one site to another site or offers a pathway for ions to be moved.[92]

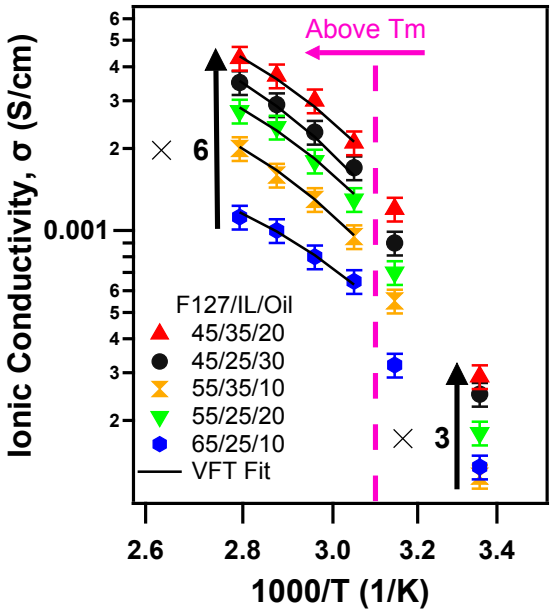

Figure 2. Temperature dependence of ionic conductivity of polymerized mesophases with different compositions. Continuous lines are fits to VTF model.

The Vogel-Tammann-Fulcher (VTF) model, eq. (2), is often used to describe the ionic conductivity in homogeneous polymer systems or heterogeneous polymer systems with fixed microstructure:[93]

$$\sigma_{VTF}(T) = \sigma_0 \exp\left(\frac{-B}{T - T_0}\right) \quad (2)$$

where $\sigma_{VTF}(T)$ is the VTF fit to the conductivity as a function of temperature T, σ_0 is the theoretical conductivity at an infinite temperature, B is a pseudoactivation energy term for ion transport, and T_0 is the Vogel temperature which is 45 ºC above the glass transition of the polymer. Sometimes, the glass transition of polymer electrolytes is not detectable by DSC scans. For example, Wanakule et al. studied the ion conductivity of mixtures of poly(styrene-block-ethylene oxide) copolymers and lithium bis(trifluoromethylsulfonimide) and were not able to detect the glass transition of samples.[94] We observed a similar phenomenon in our samples. Therefore, similar to the work by Wanakule et al.,[94] we left the

T_0 floating in the VTF model fitting to account for the shift in the glass transition. The parameters B and σ_0 obtained from the fits are shown in Table S2. The activation energy B from VTF equation provides information on the barriers associated with the conductivity. By decreasing the temperature, the polymer segmental dynamic slows down, and the dielectric constant is anticipated to increase. The segmental dynamic affects the mobility of the free ions, while the dielectric constant influences the formation of ion aggregates and the population of mobile ions as a function of temperature.

Effect of Crystallinity

A major concern for PEO-based electrolytes is poor conductivity arising from high PEO crystallinity.[95] Therefore, polymer crystallization must be prevented to achieve high ionic conductivity in polymer electrolytes. It has been shown that imidazolium-based ILs form strong interaction with the PEO block of PEO-PPO-PEO triblock copolymers, possibly through hydrogen bonding.[67] There are other works which have also shown that ILs can suppress the crystallization of hydrophilic or hydrophobic polymers.[67,96–98] Table 1 summarize the DSC results for the gel polymer electrolytes and homogeneous mixture of PEO/IL with different compositions.

The crystallinity of PEO block in neat F127 and PEO homopolymer is 77 and 87 %, respectively (the highest among all samples). Clearly, the lower crystallinity in PEO block of F127 is due to the presence of PPO middle block that hinders the organization of PEO chains in their crystalline unit cell. In ternary mesophases, the crystallinity is greater for samples having higher PEO fraction, indicating less suppression in the crystallization in these systems (46, 44, and 38 % crystallinity for mesophases with 65, 55, and 45 wt%

Pluronic, respectively). The lowest and highest crystallinity degrees (21 and 46 %) for ion gels are observed for samples with composition of F127/IL/oil 45/35/20 and 65/25/10 wt%, respectively. The WAXS results also confirm the degree of crystallinity obtained from the DSC measurements for the ion gels (Table S1). Figure 2 shows that the conductivity at room temperature (25 °C) improves by a factor of 3 for the sample with the highest to the one with the lowest crystallinity degree.

Table 1. Thermal properties of the samples from DSC experiments and tortuosity factor obtained from eq. (4)

Composition (wt%)	Crystallinity degree (%)	Melting point (°C)	Tortuosity factor at 85 °C (τ)
F127/IL/oil (65/25/10)	46±2	47	4.3
F127/IL/oil (55/25/20)	44±2	45	3.4
F127/IL/oil (45/25/30)	38±2	45	2.7
F127/IL/oil (55/35/10)	45±2	46	2.1
F127/IL/oil (45/35/20)	21±2	40	2.8
F127/IL (65/25)	62±2	48	1.2
F127/IL (45/35)	19±2	46	1.1
PEO/IL (39/25)	60±2	49	-
PEO/IL (32/25)	54±2	47	-
PEO/IL (39/35)	56±2	48	-
PEO/IL (32/35)	50±2	45	-
F127(M_W=12.6 Kg/mole)	77±2	54	-
PEO (M_W=4 Kg/mole)	87±2	60	-

Effect of Morphology

The conductivity of polymer electrolytes remarkably improves by a factor of 6 at 85 °C. The DSC results (Figure S4) show that all crystalline domains in PEO are melted at 85 °C. As control study, we measure the conductivity of homogeneous polymer electrolytes with the same ratio of PEO/IL as the mesophases at different temperatures (Figure 3a).

It is found that the conductivity of the homogeneous polymer electrolytes is lower than the mesophase systems at room temperature, while at high temperatures the opposite trend is present. Therefore, there are other factors in the polymerized mesophases systems that significantly control the conductivity of the polymer electrolytes at high temperatures. The observations can be explained by tortuosity, which is induced by two factors: crystalline domain and LLC structure. Eq. (3)[99] is employed for normalization of conductivity, where $\sigma_{ion\ gel}$ is the conductivity of polymerized mesophases, σ_h is the conductivity of the homogeneous electrolyte, and ϕ_c is the volume fraction of conducting domains in ion gels:

$$\sigma_{nor} = \frac{\sigma_{ion\ gel}}{\phi_c \sigma_h} \quad (3)$$

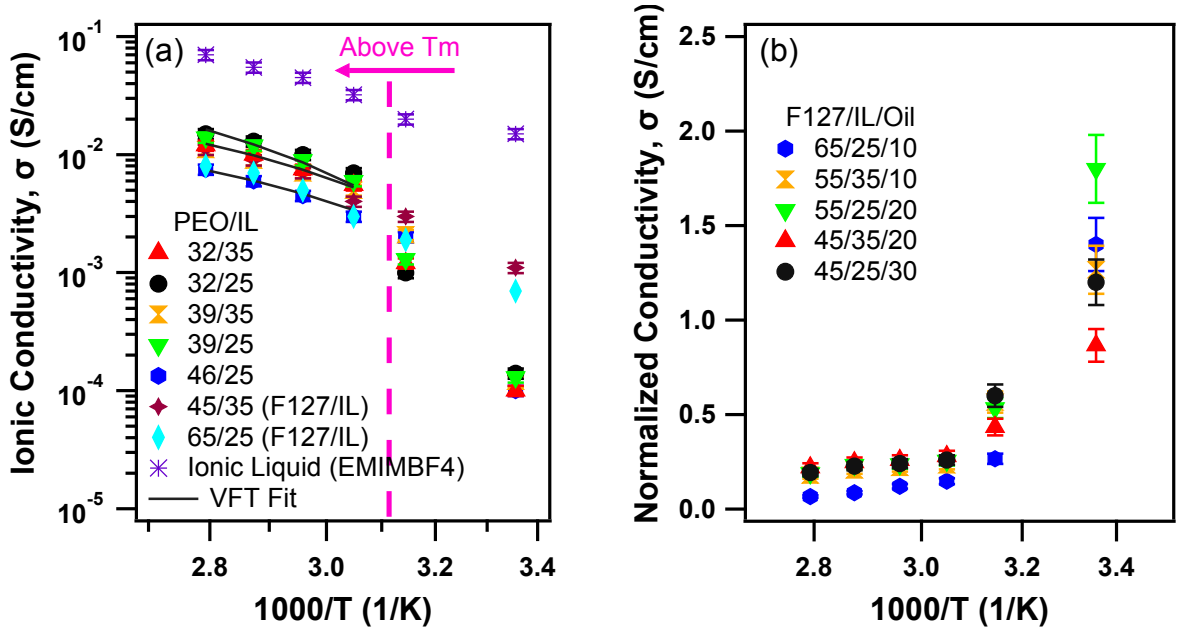

Figure 3. Temperature dependence of (a) ionic conductivity of polymer electrolytes and (b) normalized ionic conductivity of polyLLCs. Continuous lines are fits to VTF model.

The σ_{nor} value is predicted to be 1 if there is no obstruction of ion transport across the conducting phases. However, as show in Figure 3b, the normalized conductivity is higher than 1 at room temperature. As the temperature reaches the melting point of PEO, the normalized conductivity converges to values less than 1. This deviation in normalized conductivity at room temperature is because of the tortuous path induced by the crystalline domains. The tortuosity of homogeneous electrolytes (due to crystalline domains) at room temperature is obtained by extrapolation of amorphous PEO/IL conductivity, $\sigma_{\text{am. PEO/IL}}$, Figure 4.

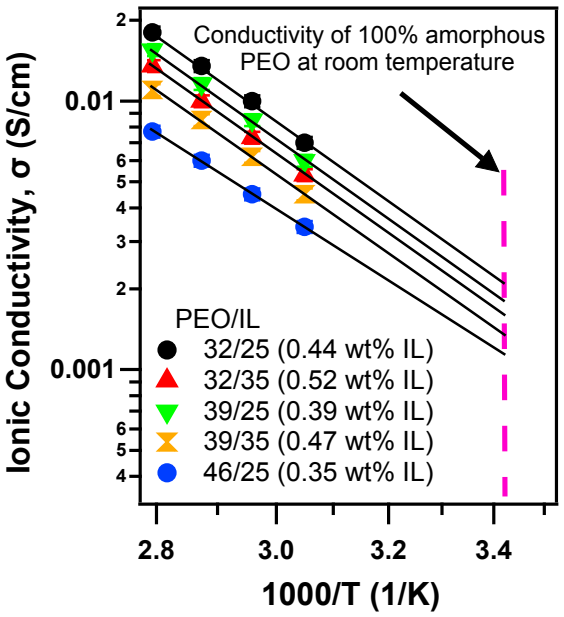

Figure 4. VTF Fitting of temperature dependent conductivity above T_m.

The room temperature conductivity for 100% amorphous PEO/IL ion gel cannot experimentally be obtained but can be extrapolated from temperature dependent conductivity above its T_m.[100] The tortuosity factor induced by crystalline domains, τ_c, for the homogenous PEO/IL was obtained from the following equation and listed in Table 2:

$$\sigma_{\text{PEO/IL}} = \sigma_{\text{am. PEO/IL}} \frac{\text{Xc}}{\tau_c} \quad (4)$$

where $\sigma_{\text{am. PEO/IL}}$ is the same as the conductivity of the homogeneous electrolyte, σ_h, and Xc is the crystallinity degree of the PEO.

Table 2. Tortuosity factor induced by crystalline domains in the homogenous PEO/IL electrolyte.

Composition (wt%)	Tortuosity factor at room temperature ($\boldsymbol{\tau_c}$)
PEO/IL (46/25) (35 wt% IL)	7.5
PEO/IL (39/25) (39 wt% IL)	7.3
PEO/IL (32/25) (44 wt% IL)	6.1
PEO/IL (39/35) (47 wt% IL)	3.9
PEO/IL (32/35) (52 wt% IL)	3.6

It is observed that high tortuosity induced by crystalline domains in the homogeneous electrolytes leads to high normalized conductivity in the ion gels. For example, the tortuosity factors for PEO/IL with ratios of 39/25 and 32/35 wt% are 7.5 and 3.6 (Table 2), respectively, which leads to highest and lowest normalized conductivity in the ion gels having the same ratio of PEO/IL, i.e., F127/IL/oil with ratios of 55/25/20 and 45/35/10 wt% with normalized conductivity of 1.8 and 0.9, respectively (Figure 3b).

As shown in Figure 3b, at 85 °C, there is a significant difference between the highest and lowest values of normalized conductivity which are 0.23 and 0.10, respectively. As mentioned earlier, at this temperature there is no crystallinity in the systems (Figure S4). Therefore, this difference in normalized conductivity at high temperatures can be attributed to two different terms; the tortuosity of the conducting nanochannels and the segmental motion of PEO blocks. The following equation is used to measure the extent of connectivity in the conducting nanochannels at 85 °C:[101]

$$\sigma_{\text{ion gel}} = \sigma_{\text{h}} \frac{\phi_{\text{c}}}{\tau} \quad (5)$$

where τ is the tortuosity factor. The tortuosity factors obtained from eq. (5) are listed in Table 1. The highest tortuosity factor (4.3) belongs to the samples with the lowest conductivity and on the other hand samples with the highest conductivity has the lowest tortuosity factor (2.1). Thus, the tortuosity plays a significant role in determining the final conductivity of the polymerized mesophases.

Segmental motion of PEO chains

The conduction in polymer electrolytes takes place through charge migration of ions between coordinated sites of the polymer along with the segmental relaxation of polymer. Dielectric relaxation is a result of the reorientation process of dipoles in the polymer chains, which shows a shoulder in ε'' spectra.[102] By increasing the temperature, the peak in ε'' spectra shifts to higher frequency suggesting the acceleration of the relaxation process[102] (Figure 5 and Figure S1).

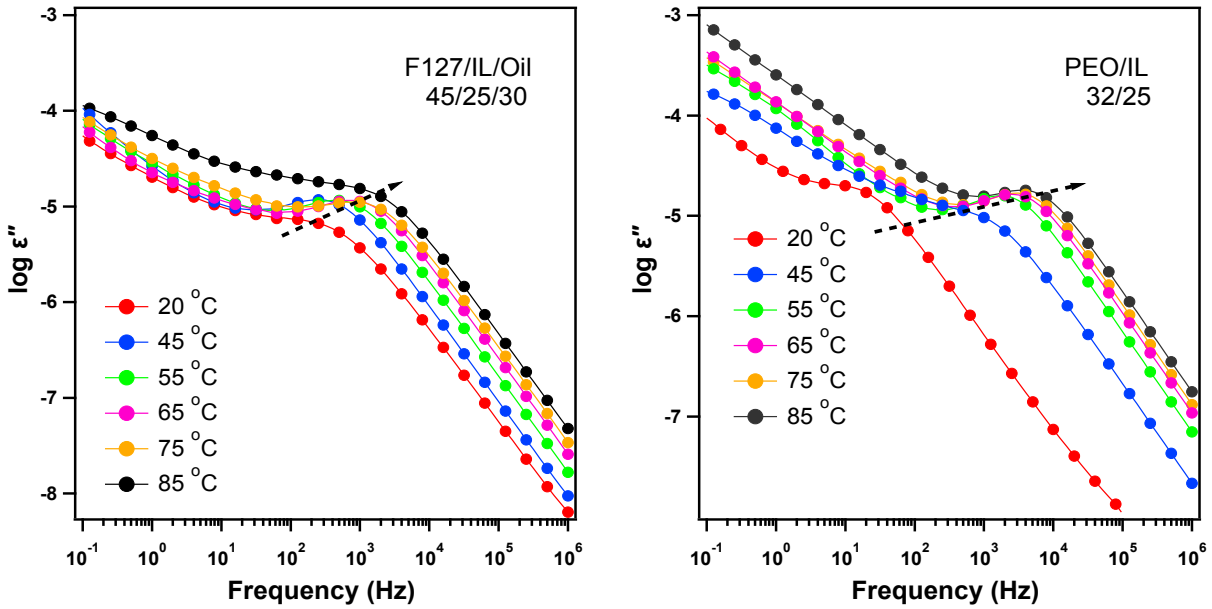

Figure 5. The dependence of dielectric loss spectra $\varepsilon''(\omega)$ on temperature for homogenous and heterogenous gel polymer electrolytes with same ratio of PEO/IL.

The complex permittivity spectra of the mesophases and homopolymers are analyzed utilizing the empirical Havriliak-Negami (HN) function:

$$\varepsilon^*(\omega) = \varepsilon_\infty + \frac{\Delta\varepsilon}{\left[1 + (i\omega\tau_{HN})^\alpha\right]^\beta} \quad (6)$$

where τ_{HN} is the characteristic relaxation time , and ω is frequency. $\Delta\varepsilon = \varepsilon_0 - \varepsilon_\infty$ is the dielectric relaxation strength of the process in which $\varepsilon_0 = \lim_{\omega\to 0} \varepsilon'(\omega)$ and $\varepsilon_\infty = \lim_{\omega\to\infty} \varepsilon'(\omega)$. The parameters α and β $(0 < \alpha,\ \alpha\beta \leq 1)$ describe the symmetric and asymmetric broadening of the distribution, respectively. The dielectric relaxation strength of the process is determined from the step-like decrease of the real permittivity data. Then, the relaxation time is obtained by fitting the imaginary part of the Havriliak/Negami equation with the imaginary permittivity data. Figure 6 shows that the relaxation time of PEO chains are different in the mesophase system with different composition and it is longer compared to the homogeneous of PEO/IL systems. Therefore, one of the factors that can explain the difference in conductivity at 85 °C (where there is no effect of crystallinity) is the difference in the relaxation time of PEO chains.

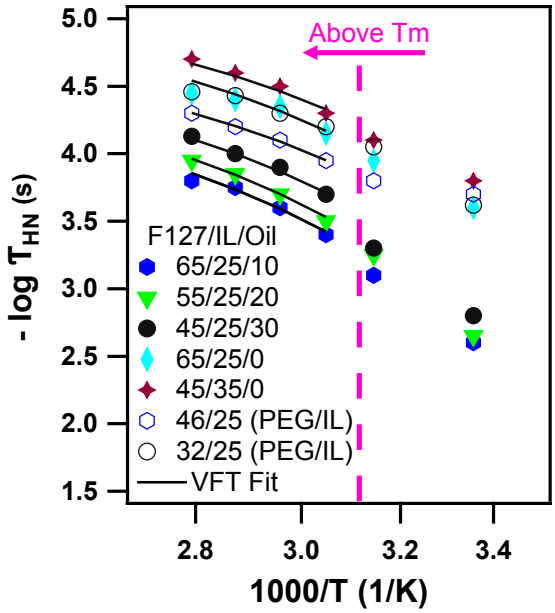

Figure 6. The temperature dependence of relaxation time for heterogeneous polymer electrolytes with formulation of F127/IL/oil wt% and homogeneous polymer electrolytes with formulation of PEO/IL wt%. Continuous lines are fits to VTF model.

With the increase of temperature, the dielectric strength of the electrolyte increases while the relaxation time becomes shorter (Figure 5 and Figure S1), which confirm the enhancement of ionic polarization with increase of temperature.[103] Mostly in polymer electrolytes, the ionic conductivity occurs in the presence of local segmental motions of the polymer host, which is due to a direct coupling between cations and functional group of the polymer.[104] Since crosslinking of the styrene restricts the molecular mobility, it is reasonable to assume that the relaxation peak of polystyrene appear at higher temperature (>100 °C) corresponding to larger activation energy.[105] PEO exhibits a VTF relaxation (α) process attributed to large-scale cooperative segmental motion of PEO chains above its melting point. The Rouse model predicts that the relaxation time for a chain with one end tethered is four times longer than that of the non-tethered chain.[106]

This can be the reason for the longer relaxation time of PEO block in mesophases (with the factor of 3.2) compared to the PEO homopolymer in homogeneous systems. Additionally, the relaxation of PEO in the mesophases becomes longer with increasing the Pluronic concentration, which can be attributed to the packing density of PEO chains in the conductive domains.

Mechanical Strength

For measuring the mechanical strength of ion gels, the mesophases have been polymerized under the rheometer by using time test in small amplitude oscillatory shear mode in linear viscoelastic region at fixed frequency (1 Hz) and strain (0.5 %) under isothermal condition (at 70 °C) (Figure 7). The results show that all ion gels have solid-like behavior, where elastic modulus is higher than loss modulus in the whole range of studied frequencies.[107] The chemorheology plot (Figure 7) shows that the mechanical strength increases between 1 to 4 orders of magnitude after polymerizing the mesophases.

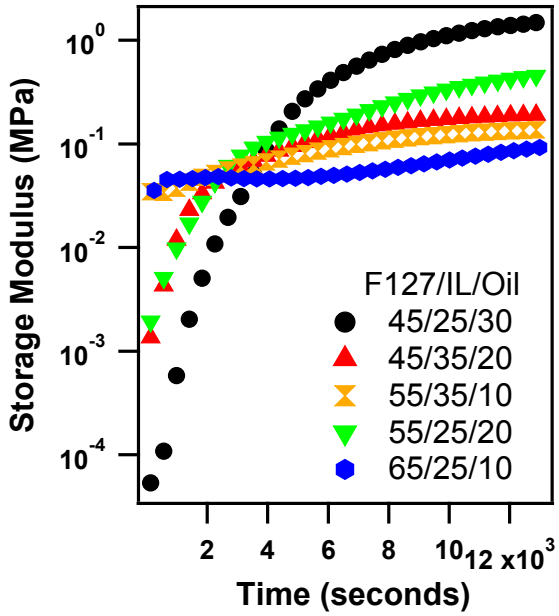

Figure 7. Evolution of storage modulus of mesophase systems with different compositions curing at 70 °C under 0.5% strain and 1 Hz frequency.

In Figure 8a, the mechanical strength of samples was plotted versus conductivity at 70 °C. As seen, the chemically cross-linked nonconductive domains of the polymer electrolytes enhance the mechanical properties in comparison to analogous block copolymer systems (45/35/0 and 65/25/0). From these results, it can be concluded that there is an optimum for the composition of mesophases to have a polymer gel electrolyte with high mechanical strength and conductivity. Additionally, increasing the ionic liquid in the system by keeping the oil concentration constant (65/25/10 versus 55/35/10) leads to higher values of conductivity without significant effect on the final mechanical strength of the system. However, increasing the oil phase while keeping the amount of ionic liquid constant (65/25/10 versus 45/25/30) enhances both the conductivity and mechanical strength. In addition, the mechanical strength and conductivity of the mesophases before and after polymerization have been compared with the ion gels prepared with PEO and

F127 (Figure 8b). The results show that the unpolymerized mesophases and homogeneous PEO samples lose their mechanical strength by increasing the temperature (red and pink markers and arrows). However, the polymerized mesophases and ion gels prepared with F127 retain their mechanical strength at high temperatures (blue and green markers and arrows). The F127/IL system almost retains the mechanical strength up to 70 °C (green markers in Figure 8b), although it has about 1 order of magnitude lower strength than analogous polyLLC (blue markers in Figure 8b). The thermal stability of the ion gels was studied using thermogravimetric analysis under nitrogen atmosphere. The samples exhibit excellent thermal stability up to 350 °C (Figure S2).

In Figure 8a, one may notice the high mechanical strength of the polymer electrolytes prepared through PIPS reported in the literature.[82] In that work, 1-butyl 3 methylimidazolium bis(trifluoromethylsulfonyl)imide, [BMI][TFSI], was used as ionic liquid which has a high ionic diffusion coefficient because of [TFSI] anion. There is also a polymer electrolyte with higher mechanical strength compared to our samples which is prepared by in situ polymerization of vinyl monomers in room temperature molten salts.[33] It should be noted that using mesophase templating method for preparation of polymer gel electrolyte provides the opportunity to control the nanostructures of the conductive and nonconductive domains separately. In addition, the chemical structure of conductive and nonconductive domains can be designed almost independently. These features are crucial for designing ion gels for applications which require highly ordered nanochannels such as membranes.

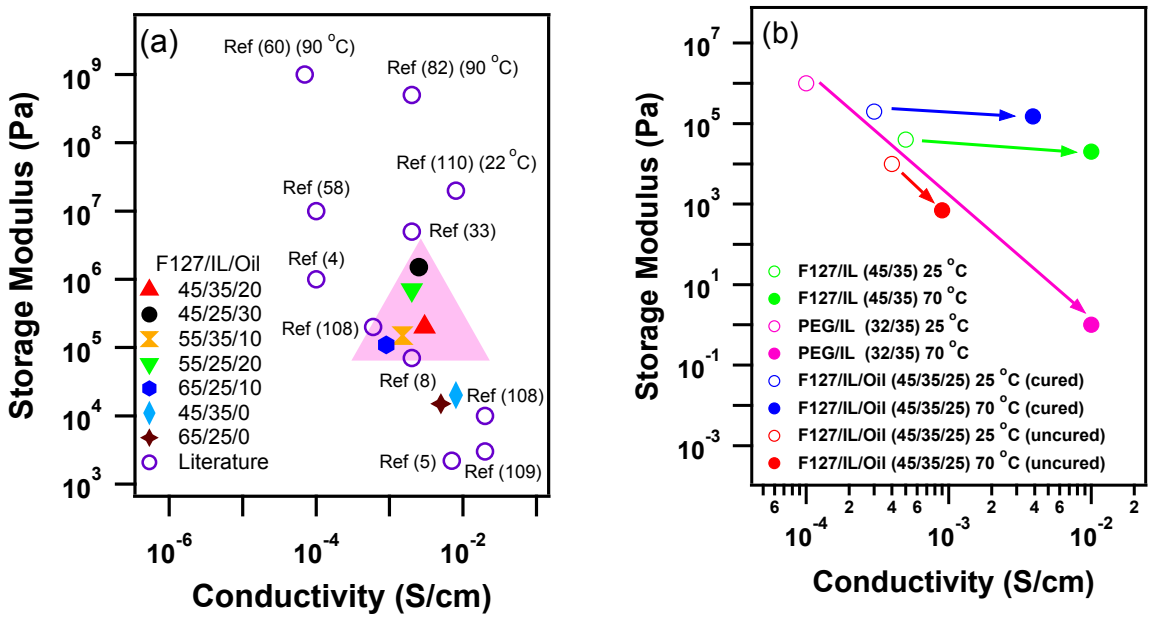

Figure 8. (a) Trade-off relationship between mechanical strength and ionic conductivity for ion gels from this study and data from literatures.[4,5,8,33,58,60,82,108–110] *All data are reported at 70 °C unless otherwise noted. (b) Mechanical strength and ionic conductivity for ion gels prepared from polyLLCs, F127/IL, and PEO/IL.*

Conclusion

We introduced a facile synthetic approach to design ion gels that exhibit high mechanical strength without compromising ionic conductivity. The outstanding bulk performance was enabled by the continuity of the conducting nanochannels and chemically cross-linked mechanical phase. It was shown that controlling the crystallinity degree of the nanochannels in lyotropic liquid crystal mesophases has significant impact in achieving an ion gel with high conductivity. The results showed that segmental relaxation of the PEO block can be controlled by sample composition. The Pluronic concentration affects its chain density at the interface and consequently the segmental motion of the PEO block

in polyLLCs, which significantly affects the final conductivity of the ion gels. Comparing our results with the data in the literature elucidated that polyLLCs offer appropriate mechanical strength and ionic conductivity with minimal need for synthesis of new amphiphilic block copolymers. In addition to the high modulus and conductivity, we introduced a versatile synthesis strategy for ion gels, which can be used in other applications where ordered heterogeneous morphology and independent tunability of the mechanical and conducting phase are desirable.

Acknowledgement

This research is supported by NM NASA EPSCoR Research Infrastructure Development (RID), Grant Number: NNX15AK41A. We would like to thank Prof. Timothy Lodge and reviewers for their comments related to SAXS results discussion.

Conflict of interest

The authors declare that they have no conflicts of interest.

References

(1) Kazarian, S. G.; Briscoe, B. J.; Welton, T. Combining Ionic Liquids and Supercritical Fluids: In Situ ATR-IR Study of CO2 Dissolved in Two Ionic Liquids at High Pressures. *Chem. Commun.* **2000**, No. 20, 2047–2048. https://doi.org/10.1039/B005514J.

(2) Huddleston, J. G.; Visser, A. E.; Reichert, W. M.; Willauer, H. D.; Broker, G. A.; Rogers, R. D. Characterization and Comparison of Hydrophilic and Hydrophobic Room Temperature Ionic Liquids Incorporating the Imidazolium Cation. *Green Chem.* **2001**, *3* (4), 156–164. https://doi.org/10.1039/B103275P.

(3) Galiński, M.; Lewandowski, A.; Stępniak, I. Ionic Liquids as Electrolytes. *Electrochim. Acta* **2006**, *51* (26), 5567–5580. https://doi.org/10.1016/j.electacta.2006.03.016.

(4) Susan, M. A. B. H.; Kaneko, T.; Noda, A.; Watanabe, M. Ion Gels Prepared by in Situ Radical Polymerization of Vinyl Monomers in an Ionic Liquid and Their Characterization as Polymer Electrolytes. *J. Am. Chem. Soc.* **2005**, *127* (13), 4976–4983. https://doi.org/10.1021/ja045155b.

(5) He, Y.; Boswell, P. G.; Bühlmann, P.; Lodge, T. P. Ion Gels by Self-Assembly of a Triblock Copolymer in an Ionic Liquid. *J. Phys. Chem. B* **2007**, *111* (18), 4645–4652. https://doi.org/10.1021/jp064574n.

(6) Klingshirn, M. A.; Spear, S. K.; Subramanian, R.; Holbrey, J. D.; Huddleston, J. G.; Rogers, R. D. Gelation of Ionic Liquids Using a Cross-Linked Poly (Ethylene Glycol) Gel Matrix. *Chem. Mater.* **2004**, *16* (16), 3091–3097. https://doi.org/10.1021/cm0351792.

(7) Ueki, T.; Watanabe, M. Macromolecules in Ionic Liquids: Progress, Challenges, and Opportunities. *Macromolecules* **2008**, *41*, 3739. https://doi.org/10.1021/ma800171k.

(8) Zhang, S.; Lee, K. H.; Frisbie, C. D.; Lodge, T. P. Ionic Conductivity, Capacitance, and Viscoelastic Properties of Block Copolymer-Based Ion Gels. *Macromolecules* **2011**, *44* (4), 940–949. https://doi.org/10.1021/ma102435a.

(9) Zhang, S.; Lee, K. H.; Sun, J.; Frisbie, C. D.; Lodge, T. P. Viscoelastic Properties, Ionic Conductivity, and Materials Design Considerations for Poly(Styrene-b-Ethylene Oxide-b-Styrene)-Based Ion Gel Electrolytes. *Macromolecules* **2011**, *44* (22), 8981–8989. https://doi.org/10.1021/ma201356j.

(10) Lee, K. H.; Zhang, S.; Lodge, T. P.; Frisbie, C. D. Electrical Impedance of Spin-Coatable Ion Gel Films. *J. Phys. Chem. B* **2011**, *115* (13), 3315–3321. https://doi.org/10.1021/jp110166u.

(11) Noro, A.; Matsushita, Y.; Lodge, T. P. Thermoreversible Supramacromolecular Ion Gels via Hydrogen Bonding. *Macromolecules* **2008**, *41* (15), 5839–5844.

https://doi.org/10.1021/ma800739c.

(12) Lei, Y.; Lodge, T. P. Effects of Component Molecular Weight on the Viscoelastic Properties of Thermoreversible Supramolecular Ion Gels via Hydrogen Bonding. *Soft Matter* **2012**, *8* (7), 2110–2120. https://doi.org/10.1039/C2SM06652A.

(13) Dong, R.-X.; Shen, S.-Y.; Chen, H.-W.; Wang, C.-C.; Shih, P.-T.; Liu, C.-T.; Vittal, R.; Lin, J.-J.; Ho, K.-C. A Novel Polymer Gel Electrolyte for Highly Efficient Dye-Sensitized Solar Cells. *J. Mater. Chem. A* **2013**, *1* (29), 8471–8478. https://doi.org/10.1039/C3TA11331K.

(14) Gorlov, M.; Kloo, L. Ionic Liquid Electrolytes for Dye-Sensitized Solar Cells. *Dalt. Trans.* **2008**, No. 20, 2655–2666. https://doi.org/10.1039/B716419J.

(15) Lee, J.; Panzer, M. J.; He, Y.; Lodge, T. P.; Frisbie, C. D. Ion Gel Gated Polymer Thin-Film Transistors. *J. Am. Chem. Soc.* **2007**, *129* (15), 4532–4533. https://doi.org/10.1021/ja070875e.

(16) Cho, J. H.; Lee, J.; He, Y.; Kim, B.; Lodge, T. P.; Frisbie, C. D. High-Capacitance Ion Gel Gate Dielectrics with Faster Polarization Response Times for Organic Thin Film Transistors. *Adv. Mater.* **2008**, *20* (4), 686–690. https://doi.org/10.1002/adma.200701069.

(17) Choi, J.-H.; Gu, Y.; Hong, K.; Xie, W.; Frisbie, C. D.; Lodge, T. P. High Capacitance, Photo-Patternable Ion Gel Gate Insulators Compatible with Vapor Deposition of Metal Gate Electrodes. *ACS Appl. Mater. Interfaces* **2014**, *6* (21), 19275–19281. https://doi.org/10.1021/am505298q.

(18) Cho, J. H.; Lee, J.; Xia, Y.; Kim, B.; He, Y.; Renn, M. J.; Lodge, T. P.; Frisbie, C. D. Printable Ion-Gel Gate Dielectrics for Low-Voltage Polymer Thin-Film Transistors on Plastic. *Nat. Mater.* **2008**, *7*, 900. https://doi.org/10.1038/nmat2291.

(19) Kim, S. H.; Hong, K.; Xie, W.; Lee, K. H.; Zhang, S.; Lodge, T. P.; Frisbie, C. D. Electrolyte-Gated Transistors for Organic and Printed Electronics. *Adv. Mater.* **2013**, *25* (13), 1822–1846. https://doi.org/10.1002/adma.201202790.

(20) Lee, J.; Kaake, L. G.; Cho, J. H.; Zhu, X.-Y.; Lodge, T. P.; Frisbie, C. D. Ion Gel-Gated

Polymer Thin-Film Transistors: Operating Mechanism and Characterization of Gate Dielectric Capacitance, Switching Speed, and Stability. *J. Phys. Chem. C* **2009**, *113* (20), 8972–8981. https://doi.org/10.1021/jp901426e.

(21) Kim, B. J.; Lee, S.-K.; Kang, M. S.; Ahn, J.-H.; Cho, J. H. Coplanar-Gate Transparent Graphene Transistors and Inverters on Plastic. *ACS Nano* **2012**, *6* (10), 8646–8651. https://doi.org/10.1021/nn3020486.

(22) Thiemann, S.; Sachnov, S. J.; Pettersson, F.; Bollström, R.; Österbacka, R.; Wasserscheid, P.; Zaumseil, J. Cellulose-Based Ionogels for Paper Electronics. *Adv. Funct. Mater.* **2014**, *24* (5), 625–634. https://doi.org/10.1002/adfm.201302026.

(23) Choi, Y.; Kang, J.; Jariwala, D.; Kang, M. S.; Marks, T. J.; Hersam, M. C.; Cho, J. H. Low-Voltage Complementary Electronics from Ion-Gel-Gated Vertical Van Der Waals Heterostructures. *Adv. Mater.* **2016**, *28* (19), 3742–3748. https://doi.org/10.1002/adma.201506450.

(24) Tang, B.; Schneiderman, D. K.; Zare Bidoky, F.; Frisbie, C. D.; Lodge, T. P. Printable, Degradable, and Biocompatible Ion Gels from a Renewable ABA Triblock Polyester and a Low Toxicity Ionic Liquid. *ACS Macro Lett.* **2017**, *6* (10), 1083–1088. https://doi.org/10.1021/acsmacrolett.7b00582.

(25) Moon, H. C.; Lodge, T. P.; Frisbie, C. D. DC-Driven, Sub-2 V Solid-State Electrochemiluminescent Devices by Incorporating Redox Coreactants into Emissive Ion Gels. *Chem. Mater.* **2014**, *26* (18), 5358–5364. https://doi.org/10.1021/cm502491n.

(26) Moon, H. C.; Lodge, T. P.; Frisbie, C. D. Solution-Processable Electrochemiluminescent Ion Gels for Flexible, Low-Voltage, Emissive Displays on Plastic. *J. Am. Chem. Soc.* **2014**, *136* (9), 3705–3712. https://doi.org/10.1021/ja5002899.

(27) Moon, H. C.; Kim, C.-H.; Lodge, T. P.; Frisbie, C. D. Multicolored, Low-Power, Flexible Electrochromic Devices Based on Ion Gels. *ACS Appl. Mater. Interfaces* **2016**, *8* (9), 6252–6260. https://doi.org/10.1021/acsami.6b01307.

(28) Moon, H. C.; Lodge, T. P.; Frisbie, C. D. Solution Processable, Electrochromic Ion Gels for Sub-1 V, Flexible Displays on Plastic. *Chem. Mater.* **2015**, *27* (4), 1420–1425. https://doi.org/10.1021/acs.chemmater.5b00026.

(29) Kang, Y. J.; Chun, S.-J.; Lee, S.-S.; Kim, B.-Y.; Kim, J. H.; Chung, H.; Lee, S.-Y.; Kim, W. All-Solid-State Flexible Supercapacitors Fabricated with Bacterial Nanocellulose Papers, Carbon Nanotubes, and Triblock-Copolymer Ion Gels. *ACS Nano* **2012**, *6* (7), 6400–6406. https://doi.org/10.1021/nn301971r.

(30) Yang, X.; Zhang, F.; Zhang, L.; Zhang, T.; Huang, Y.; Chen, Y. A High-Performance Graphene Oxide-Doped Ion Gel as Gel Polymer Electrolyte for All-Solid-State Supercapacitor Applications. *Adv. Funct. Mater.* **2013**, *23* (26), 3353–3360. https://doi.org/10.1002/adfm.201203556.

(31) Gu, Y.; Cussler, E. L.; Lodge, T. P. ABA-Triblock Copolymer Ion Gels for CO2 Separation Applications. *J. Membr. Sci.* **2012**, *423–424*, 20. https://doi.org/10.1016/j.memsci.2012.07.011.

(32) Gu, Y.; Lodge, T. P. Synthesis and Gas Separation Performance of Triblock Copolymer Ion Gels with a Polymerized Ionic Liquid Mid-Block. *Macromolecules* **2011**, *44* (7), 1732–1736. https://doi.org/10.1021/ma2001838.

(33) Noda, A.; Watanabe, M. Highly Conductive Polymer Electrolytes Prepared by in Situ Polymerization of Vinyl Monomers in Room Temperature Molten Salts. *Electrochim. Acta* **2000**, *45* (8), 1265–1270. https://doi.org/10.1016/S0013-4686(99)00330-8.

(34) Matsumoto, K.; Endo, T. Confinement of Ionic Liquid by Networked Polymers Based on Multifunctional Epoxy Resins. *Macromolecules* **2008**, *41* (19), 6981–6986. https://doi.org/10.1021/ma801293j.

(35) Lodge, T. P. A Unique Platform for Materials Design. *Science (80-.).* **2008**, *321*, 50. https://doi.org/10.1126/science.1159652.

(36) He, Y.; Lodge, T. P. A Thermoreversible Ion Gel by Triblock Copolymer Self-Assembly in

an Ionic Liquid. *Chem. Commun.* **2007**, No. 26, 2732–2734. https://doi.org/10.1039/B704490A.

(37) Hall, C. C.; Zhou, C.; Danielsen, S. P. O.; Lodge, T. P. Formation of Multicompartment Ion Gels by Stepwise Self-Assembly of a Thermoresponsive ABC Triblock Terpolymer in an Ionic Liquid. *Macromolecules* **2016**, *49* (6), 2298–2306. https://doi.org/10.1021/acs.macromol.5b02789.

(38) Noro, A.; Matsushita, Y.; Lodge, T. P. Gelation Mechanism of Thermoreversible Supramacromolecular Ion Gels via Hydrogen Bonding. *Macromolecules* **2009**, *42* (15), 5802–5810. https://doi.org/10.1021/ma900820g.

(39) Ueki, T.; Usui, R.; Kitazawa, Y.; Lodge, T. P.; Watanabe, M. Thermally Reversible Ion Gels with Photohealing Properties Based on Triblock Copolymer Self-Assembly. *Macromolecules* **2015**, *48* (16), 5928–5933. https://doi.org/10.1021/acs.macromol.5b01366.

(40) Tamate, R.; Hashimoto, K.; Ueki, T.; Watanabe, M. Block Copolymer Self-Assembly in Ionic Liquids. *Phys. Chem. Chem. Phys.* **2018**, *20* (39), 25123–25139. https://doi.org/10.1039/C8CP04173C.

(41) Zhu, Y.; Wang, F.; Liu, L.; Xiao, S.; Chang, Z.; Wu, Y. Composite of a Nonwoven Fabric with Poly(Vinylidene Fluoride) as a Gel Membrane of High Safety for Lithium Ion Battery. *Energy Environ. Sci.* **2013**, *6* (2), 618–624. https://doi.org/10.1039/C2EE23564A.

(42) Hallinan, D. T.; Balsara, N. P. Polymer Electrolytes. *Annu. Rev. Mater. Res.* **2013**, *43* (1), 503–525. https://doi.org/10.1146/annurev-matsci-071312-121705.

(43) Bates, F. S.; Fredrickson, G. H. Block Copolymers-Designer Soft Materials. *Phys. Today* **2000**, *52*. https://doi.org/10.1063/1.882522.

(44) Matsen, M. W.; Bates, F. S. Unifying Weak- and Strong-Segregation Block Copolymer Theories. *Macromolecules* **1996**, *29* (4), 1091–1098. https://doi.org/10.1021/ma951138i.

(45) Hoarfrost, M. L.; Tyagi, M. S.; Segalman, R. A.; Reimer, J. A. Effect of Confinement on

Proton Transport Mechanisms in Block Copolymer/Ionic Liquid Membranes. *Macromolecules* **2012**, *45* (7), 3112–3120. https://doi.org/10.1021/ma202741g.

(46) Virgili, J. M.; Hoarfrost, M. L.; Segalman, R. A. Effect of an Ionic Liquid Solvent on the Phase Behavior of Block Copolymers. *Macromolecules* **2010**, *43* (12), 5417–5423. https://doi.org/10.1021/ma902804e.

(47) Matsumoto, T.; Ichikawa, T.; Ohno, H. Design of Ionic Liquid-Based Polyelectrolytes by Combining 'Nanostructurisation' and 'Zwitterionisation.' *Polym. Chem.* **2016**, *7* (6), 1230–1233. https://doi.org/10.1039/C5PY01838B.

(48) Kitazawa, Y.; Iwata, K.; Imaizumi, S.; Ahn, H.; Kim, S. Y.; Ueno, K.; Park, M. J.; Watanabe, M. Gelation of Solvate Ionic Liquid by Self-Assembly of Block Copolymer and Characterization as Polymer Electrolyte. *Macromolecules* **2014**, *47* (17), 6009–6016. https://doi.org/10.1021/ma501296m.

(49) Miranda, D. F.; Versek, C.; Tuominen, M. T.; Russell, T. P.; Watkins, J. J. Cross-Linked Block Copolymer/Ionic Liquid Self-Assembled Blends for Polymer Gel Electrolytes with High Ionic Conductivity and Mechanical Strength. *Macromolecules* **2013**, *46* (23), 9313–9323. https://doi.org/10.1021/ma401302r.

(50) Castiglione, F.; Ragg, E.; Mele, A.; Appetecchi, G. B.; Montanino, M.; Passerini, S. Molecular Environment and Enhanced Diffusivity of Li+ Ions in Lithium-Salt-Doped Ionic Liquid Electrolytes. *J. Phys. Chem. Lett.* **2011**, *2* (3), 153–157. https://doi.org/10.1021/jz101516c.

(51) Simone, P. M.; Lodge, T. P. Phase Behavior and Ionic Conductivity of Concentrated Solutions of Polystyrene-Poly(Ethylene Oxide) Diblock Copolymers in an Ionic Liquid. *ACS Appl. Mater. Interfaces* **2009**, *1* (12), 2812–2820. https://doi.org/10.1021/am900555f.

(52) Weber, R. L.; Ye, Y.; Schmitt, A. L.; Banik, S. M.; Elabd, Y. A.; Mahanthappa, M. K. Effect of Nanoscale Morphology on the Conductivity of Polymerized Ionic Liquid Block

Copolymers. *Macromolecules* **2011**, *44* (14), 5727–5735. https://doi.org/10.1021/ma201067h.

(53) Cho, B.-K.; Jain, A.; Gruner, S. M.; Wiesner, U. Mesophase Structure-Mechanical and Ionic Transport Correlations in Extended Amphiphilic Dendrons. *Science (80-.).* **2004**, *305* (5690), 1598 LP – 1601. https://doi.org/10.1126/science.1100872.

(54) Kim, O.; Kim, S. Y.; Lee, J.; Park, M. J. Building Less Tortuous Ion-Conduction Pathways Using Block Copolymer Electrolytes with a Well-Defined Cubic Symmetry. *Chem. Mater.* **2016**, *28* (1), 318–325. https://doi.org/10.1021/acs.chemmater.5b04157.

(55) Kim, O.; Kim, S. Y.; Ahn, H.; Kim, C. W.; Rhee, Y. M.; Park, M. J. Phase Behavior and Conductivity of Sulfonated Block Copolymers Containing Heterocyclic Diazole-Based Ionic Liquids. *Macromolecules* **2012**, *45* (21), 8702–8713. https://doi.org/10.1021/ma301803f.

(56) Kim, O.; Jo, G.; Park, Y. J.; Kim, S.; Park, M. J. Ion Transport Properties of Self-Assembled Polymer Electrolytes: The Role of Confinement and Interface. *J. Phys. Chem. Lett.* **2013**, *4* (13), 2111–2117. https://doi.org/10.1021/jz4009536.

(57) Panday, A.; Mullin, S.; Gomez, E. D.; Wanakule, N.; Chen, V. L.; Hexemer, A.; Pople, J.; Balsara, N. P. Effect of Molecular Weight and Salt Concentration on Conductivity of Block Copolymer Electrolytes. *Macromolecules* **2009**, *42* (13), 4632–4637. https://doi.org/10.1021/ma900451e.

(58) Green, M. D.; Choi, J.-H.; Winey, K. I.; Long, T. E. Synthesis of Imidazolium-Containing ABA Triblock Copolymers: Role of Charge Placement, Charge Density, and Ionic Liquid Incorporation. *Macromolecules* **2012**, *45* (11), 4749–4757. https://doi.org/10.1021/ma300185b.

(59) Choi, J.-H.; Ye, Y.; Elabd, Y. A.; Winey, K. I. Network Structure and Strong Microphase Separation for High Ion Conductivity in Polymerized Ionic Liquid Block Copolymers. *Macromolecules* **2013**, *46* (13), 5290–5300. https://doi.org/10.1021/ma400562a.

(60) Singh, M.; Odusanya, O.; Wilmes, G. M.; Eitouni, H. B.; Gomez, E. D.; Patel, A. J.; Chen, V. L.; Park, M. J.; Fragouli, P.; Iatrou, H.; Hadjichristidis, N.; Cookson, D.; Balsara, N. P. Effect of Molecular Weight on the Mechanical and Electrical Properties of Block Copolymer Electrolytes. *Macromolecules* **2007**, *40* (13), 4578–4585. https://doi.org/10.1021/ma0629541.

(61) Qavi, S.; Foudazi, R. Rheological Characteristics of Mesophases of Block Copolymer Solutions. *Rheol. Acta* **2019**, *58* (8), 483–498. https://doi.org/10.1007/s00397-019-01162-y.

(62) Qavi, S.; Bandegi, A.; Firestone, M.; Foudazi, R. Polymerization in Soft Nanoconfinements of Lamellar and Reverse Hexagonal Mesophases. *Soft Matter* **2019**, *15* (41), 8238–8250. https://doi.org/10.1039/C9SM01565E.

(63) Robertson, L. A.; Schenkel, M. R.; Wiesenauer, B. R.; Gin, D. L. Alkyl-Bis(Imidazolium) Salts: A New Amphiphile Platform That Forms Thermotropic and Non-Aqueous Lyotropic Bicontinuous Cubic Phases. *Chem. Commun.* **2013**, *49* (82), 9407–9409. https://doi.org/10.1039/C3CC44452J.

(64) Hanley, K. J.; Lodge, T. P.; Huang, C.-I. Phase Behavior of a Block Copolymer in Solvents of Varying Selectivity. *Macromolecules* **2000**, *33* (16), 5918–5931. https://doi.org/10.1021/ma000318b.

(65) Lodge, T. P.; Hanley, K. J.; Pudil, B.; Alahapperuma, V. Phase Behavior of Block Copolymers in a Neutral Solvent. *Macromolecules* **2003**, *36* (3), 816–822. https://doi.org/10.1021/ma0209601.

(66) Simone, P. M.; Lodge, T. P. Lyotropic Phase Behavior of Polybutadiene−Poly(Ethylene Oxide) Diblock Copolymers in Ionic Liquids. *Macromolecules* **2008**, *41* (5), 1753–1759. https://doi.org/10.1021/ma702252v.

(67) Miranda, D. F.; Russell, T. P.; Watkins, J. J. Ordering in Mixtures of a Triblock Copolymer with a Room Temperature Ionic Liquid. *Macromolecules* **2010**, *43* (24), 10528–10535.

https://doi.org/10.1021/ma1015209.

(68) Hoag, B. P.; Gin, D. L. Cross-Linkable Liquid Crystal Monomers Containing Hydrocarbon 1,3-Diene Tail Systems. *Macromolecules* **2000**, *33* (23), 8549–8558. https://doi.org/10.1021/ma000812f.

(69) Pindzola, B. A.; Jin, J.; Gin, D. L. Cross-Linked Normal Hexagonal and Bicontinuous Cubic Assemblies via Polymerizable Gemini Amphiphiles. *J. Am. Chem. Soc.* **2003**, *125* (10), 2940–2949. https://doi.org/10.1021/ja0208106.

(70) Lester, C. L.; Guymon, C. A. Ordering Effects on the Photopolymerization of a Lyotropic Liquid Crystal. *Polymer (Guildf).* **2002**, *43* (13), 3707–3715. https://doi.org/http://dx.doi.org/10.1016/S0032-3861(02)00188-X.

(71) Lester, C. L.; Guymon, C. A. Phase Behavior and Polymerization Kinetics of a Semifluorinated Lyotropic Liquid Crystal. *Macromolecules* **2000**, *33* (15), 5448–5454. https://doi.org/10.1021/ma000197f.

(72) Gin, D. L.; Gu, W.; Pindzola, B. A.; Zhou, W.-J. Polymerized Lyotropic Liquid Crystal Assemblies for Materials Applications. *Acc. Chem. Res.* **2001**, *34* (12), 973–980. https://doi.org/10.1021/ar000140d.

(73) Lester, C. L.; Colson, C. D.; Guymon, C. A. Photopolymerization Kinetics and Structure Development of Templated Lyotropic Liquid Crystalline Systems. *Macromolecules* **2001**, *34* (13), 4430–4438. https://doi.org/10.1021/ma001853e.

(74) Lester, C. L.; Smith, S. M.; Jarrett, W. L.; Guymon, C. A. Effects of Monomer Organization on the Photopolymerization Kinetics of Acrylamide in Lyotropic Liquid Crystalline Phases. *Langmuir* **2003**, *19* (22), 9466–9472. https://doi.org/10.1021/la0300784.

(75) McCormick, D. T.; Stovall, K. D.; Guymon, C. A. Photopolymerization in Pluronic Lyotropic Liquid Crystals: Induced Mesophase Thermal Stability. *Macromolecules* **2003**, *36* (17), 6549–6558. https://doi.org/10.1021/ma030037e.

(76) Laversanne, R. Polymerization of Acrylamide in Lamellar, Hexagonal, and Cubic Lyotropic Phases. *Macromolecules* **1992**, *25* (Figure 2), 489–491. https://doi.org/10.1021/ma00027a077.

(77) Qavi, S.; Lindsay, A. P.; Firestone, M. A.; Foudazi, R. Ultrafiltration Membranes from Polymerization of Self-Assembled Pluronic Block Copolymer Mesophases. *J. Memb. Sci.* **2019**, *580*, 125–133. https://doi.org/10.1016/j.memsci.2019.02.060.

(78) Qavi, S.; Bandegi, A.; Firestone, M.; Foudazi, R. Polymerization in Soft Nanoconfinement of Lamellar and Reverse Hexagonal Mesophases. *Soft Matter* **2019**, *15* (41), 8238–8250. https://doi.org/10.1039/C9SM01565E.

(79) Qiu, Z.; Ikehara, T.; Nishi, T. Miscibility and Crystallization in Crystalline/Crystalline Blends of Poly(Butylene Succinate)/Poly(Ethylene Oxide). *Polymer (Guildf).* **2003**, *44* (9), 2799–2806. https://doi.org/10.1016/S0032-3861(03)00149-6.

(80) Kubisa, P. Ionic Liquids as Solvents for Polymerization Processes—Progress and Challenges. *Prog. Polym. Sci.* **2009**, *34* (12), 1333–1347. https://doi.org/10.1016/j.progpolymsci.2009.09.001.

(81) Zhou, N.; Lodge, T. P.; Bates, F. S. Influence of Conformational Asymmetry on the Phase Behavior of Ternary Homopolymer/Block Copolymer Blends around the Bicontinuous Microemulsion Channel. *J. Phys. Chem. B* **2006**, *110* (9), 3979–3989. https://doi.org/10.1021/jp055704f.

(82) Schulze, M. W.; McIntosh, L. D.; Hillmyer, M. A.; Lodge, T. P. High-Modulus, High-Conductivity Nanostructured Polymer Electrolyte Membranes via Polymerization-Induced Phase Separation. *Nano Lett.* **2014**, *14* (1), 122–126. https://doi.org/10.1021/nl4034818.

(83) Vidil, T.; Hampu, N.; Hillmyer, M. A. Nanoporous Thermosets with Percolating Pores from Block Polymers Chemically Fixed above the Order–Disorder Transition. *ACS Cent. Sci.* **2017**, *3* (10), 1114–1120. https://doi.org/10.1021/acscentsci.7b00358.

(84) Chen, H.-L.; Wang, S.-F. Crystallization Induced Microstructure of Polymer Blends

Consisting of Two Crystalline Constituents. *Polymer (Guildf).* **2000**, *41* (14), 5157–5164. https://doi.org/https://doi.org/10.1016/S0032-3861(99)00745-4.

(85) Schultz, J. M. Rapid Small-Angle and Wide-Angle x-Ray Studies of Crystallization Behavior in Polymers. *J. Polym. Sci. Polym. Phys. Ed.* **1976**, *14* (12), 2291–2311. https://doi.org/10.1002/pol.1976.180141214.

(86) Gebel, G.; Diat, O. Neutron and X-Ray Scattering: Suitable Tools for Studying Ionomer Membranes. *Fuel Cells* **2005**, *5* (2), 261–276. https://doi.org/10.1002/fuce.200400080.

(87) Grady, B. P.; Matsuoka, H.; Nakatani, Y.; Cooper, S. L.; Ise, N. Influence of the Sample Preparation Method of the Ultra-Small-Angle x-Ray Scattering of Lightly Sulfonated Polystyrenes. *Macromolecules* **1993**, *26* (15), 4064–4066. https://doi.org/10.1021/ma00067a055.

(88) Li, Y.; Peiffer, D. G.; Chu, B. Long-Range Inhomogeneities in Sulfonated Polystyrene Ionomers. *Macromolecules* **1993**, *26* (15), 4006–4012. https://doi.org/10.1021/ma00067a042.

(89) Ford, H. O.; Cui, C.; Schaefer, J. L. Comparison of Single-Ion Conducting Polymer Gel Electrolytes for Sodium, Potassium, and Calcium Batteries: Influence of Polymer Chemistry, Cation Identity, Charge Density, and Solvent on Conductivity. *Batteries* **2020**, *6* (1), 11. https://doi.org/10.3390/batteries6010011.

(90) Sangoro, J. R.; Iacob, C.; Agapov, A. L.; Wang, Y.; Berdzinski, S.; Rexhausen, H.; Strehmel, V.; Friedrich, C.; Sokolov, A. P.; Kremer, F. Decoupling of Ionic Conductivity from Structural Dynamics in Polymerized Ionic Liquids. *Soft Matter* **2014**, *10* (20), 3536–3540. https://doi.org/10.1039/C3SM53202J.

(91) Choi, U. H.; Ye, Y.; Salas de la Cruz, D.; Liu, W.; Winey, K. I.; Elabd, Y. A.; Runt, J.; Colby, R. H. Dielectric and Viscoelastic Responses of Imidazolium-Based Ionomers with Different Counterions and Side Chain Lengths. *Macromolecules* **2014**, *47* (2), 777–790. https://doi.org/10.1021/ma402263y.

(92) Aziz, S. B.; Woo, T. J.; Kadir, M. F. Z.; Ahmed, H. M. A Conceptual Review on Polymer Electrolytes and Ion Transport Models. *J. Sci. Adv. Mater. Devices* **2018**, *3* (1), 1–17. https://doi.org/10.1016/j.jsamd.2018.01.002.

(93) Young, W.-S.; Kuan, W.-F.; Epps Thomas H., I. I. I. Block Copolymer Electrolytes for Rechargeable Lithium Batteries. *J. Polym. Sci. Part B Polym. Phys.* **2014**, *52* (1), 1–16. https://doi.org/10.1002/polb.23404.

(94) Wanakule, N. S.; Panday, A.; Mullin, S. A.; Gann, E.; Hexemer, A.; Balsara, N. P. Ionic Conductivity of Block Copolymer Electrolytes in the Vicinity of Order−Disorder and Order−Order Transitions. *Macromolecules* **2009**, *42* (15), 5642–5651. https://doi.org/10.1021/ma900401a.

(95) Berthier, C.; Gorecki, W.; Minier, M.; Armand, M. B.; Chabagno, J. M.; Rigaud, P. Microscopic Investigation of Ionic Conductivity in Alkali Metal Salts-Poly(Ethylene Oxide) Adducts. *Solid State Ionics* **1983**, *11* (1), 91–95. https://doi.org/10.1016/j.ssi.2007.06.006.

(96) Choi, J.-W.; Cheruvally, G.; Kim, Y.-H.; Kim, J.-K.; Manuel, J.; Raghavan, P.; Ahn, J.-H.; Kim, K.-W.; Ahn, H.-J.; Choi, D. S.; Song, C. E. Poly(Ethylene Oxide)-Based Polymer Electrolyte Incorporating Room-Temperature Ionic Liquid for Lithium Batteries. *Solid State Ionics* **2007**, *178* (19), 1235–1241. https://doi.org/10.1016/j.ssi.2007.06.006.

(97) Kumar, D.; Hashmi, S. A. Ionic Liquid Based Sodium Ion Conducting Gel Polymer Electrolytes. *Solid State Ionics* **2010**, *181* (8), 416–423. https://doi.org/10.1016/j.ssi.2010.01.025.

(98) Kim, S.; Park, S.-J. Preparation and Electrochemical Properties of Composite Polymer Electrolytes Containing 1-Ethyl-3-Methylimidazolium Tetrafluoroborate Salts. *Electrochim. Acta* **2009**, *54* (14), 3775–3780. https://doi.org/10.1016/j.jiec.2009.09.039.

(99) Xie, S.; Meyer, D. J.; Wang, E.; Bates, F. S.; Lodge, T. P. Structure and Properties of Bicontinuous Microemulsions from Salt-Doped Ternary Polymer Blends. *Macromolecules* **2019**, *52* (24), 9693–9702. https://doi.org/10.1021/acs.macromol.9b01963.

(100) Cheng, S.; Smith, D. M.; Li, C. Y. How Does Nanoscale Crystalline Structure Affect Ion Transport in Solid Polymer Electrolytes? *Macromolecules* **2014**, *47* (12), 3978–3986. https://doi.org/10.1021/ma500734q.

(101) Chopade, S. A.; Au, J. G.; Li, Z.; Schmidt, P. W.; Hillmyer, M. A.; Lodge, T. P. Robust Polymer Electrolyte Membranes with High Ambient-Temperature Lithium-Ion Conductivity via Polymerization-Induced Microphase Separation. *ACS Appl. Mater. Interfaces* **2017**, *9* (17), 14561–14565. https://doi.org/10.1021/acsami.7b02514.

(102) Pradhan, D. K.; Choudhary, R. N. P.; Samantaray, B. K. Studies of Dielectric Relaxation and AC Conductivity Behavior of Plasticized Polymer Nanocomposite Electrolytes. *Int. J. Electrochem. Sci* **2008**, *3* (5), 597-608. www.electrochemsci.org/papers/vol3/305059.

(103) Sengwa, R. J.; Choudhary, S. Dielectric Relaxation Spectroscopy and X-Ray Diffraction Studies of Poly (Ethylene Oxide)–Lithium Perchlorate Electrolytes. *Indian J. Phys.* **2014**, *88* (5), 461–470. https://doi.org/10.1007/s12648-014-0440-7.

(104) Choudhary, S.; Sengwa, R. J. Effects of Preparation Methods on Structure, Ionic Conductivity and Dielectric Relaxation of Solid Polymeric Electrolytes. *Mater. Chem. Phys.* **2013**, *142* (1), 172–181. https://doi.org/10.1016/j.matchemphys.2013.06.053.

(105) Aras, L.; Baysal, B. M. Dielectric Relaxation Studies of Some Linear Crosslinked and Branched Polymers. *J. Polym. Sci. Polym. Phys. Ed.* **1984**, *22* (8), 1453–1460. https://doi.org/10.1002/pol.1984.180220809.

(106) Adachi, K.; Kotaka, T. Dielectric Normal Mode Relaxation of Tethered Polyisoprene Chains in Styrene-Isoprene Block Copolymers. *Pure Appl. Chem.* **1997**, *69* (1), 125–130. https://doi.org/10.3390/polym7071346.

(107) Foudazi, R.; Qavi, S.; Masalova, I.; Malkin, A. Y. Physical Chemistry of Highly Concentrated Emulsions. *Adv. Colloid Interface Sci.* **2015**, *220*, 78–91. https://doi.org/10.1016/j.cis.2015.03.002.

(108) Tang, B.; White, S. P.; Frisbie, C. D.; Lodge, T. P. Synergistic Increase in Ionic

Conductivity and Modulus of Triblock Copolymer Ion Gels. *Macromolecules* **2015**, *48* (14), 4942–4950. https://doi.org/10.1021/acs.macromol.5b00882.

(109) Lee, K. H.; Zhang, S.; Gu, Y.; Lodge, T. P.; Frisbie, C. D. Transfer Printing of Thermoreversible Ion Gels for Flexible Electronics. *ACS Appl. Mater. Interfaces* **2013**, *5* (19), 9522–9527. https://doi.org/10.1021/am402200n.

(110) Wang, Y.; Chen, Y.; Gao, J.; Yoon, H. G.; Jin, L.; Forsyth, M.; Dingemans, T. J.; Madsen, L. A. Highly Conductive and Thermally Stable Ion Gels with Tunable Anisotropy and Modulus. *Adv. Mater.* **2016**, *28* (13), 2571–2578. https://doi.org/10.1002/adma.201505183.

849

850 **"For Table of Contents Only"**

851 **Formation of Ion Gels by Polymerization of Block Copolymer/Ionic Liquid/Oil**

852 **Mesophases**

853 Alireza Bandegi [a], Jose L. Bañuelos [b], Reza Foudazi [a]

854 [a] Department of Chemical and Materials Engineering, New Mexico State University, Las

855 Cruces, NM, 88003, United States

856 [b] Department of Physics, The University of Texas at El Paso, El Paso, TX, 79968, United

857 States

858

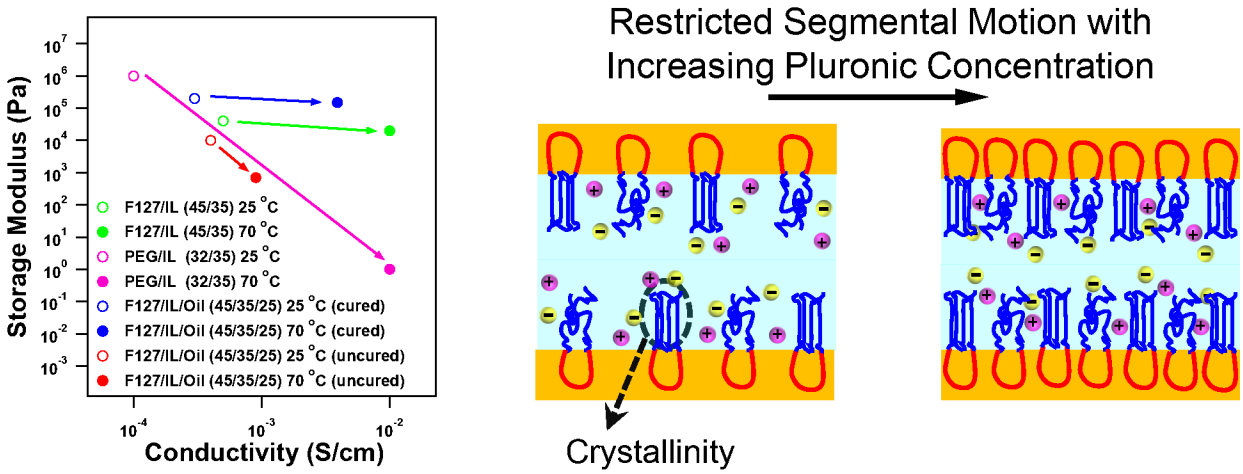

859

860 **Keywords:** Ion gel, Ionic Conductivity, Mechanical Strength, Crystallinity, Segmental

861 Motion.